JOURNAL OF THERMOPHYSICS AND HEAT TRANSFER
Vol. 21, No. 2, April–June 2007

Heating of Finite Slabs Subjected to Laser Pulse Irradiation and Convective Cooling

T. K. Cheung,* B. A. Blake,† and T. T. Lam‡
The Aerospace Corporation, Los Angeles, California 90009-2957

DOI: 10.2514/1.23100

An analytical solution was obtained for one-dimensional heat conduction within a finite region that was subjected to a realistic laser pulse profile. The results provide an improved model of laser heating at a surface by combining a spatially and temporally decaying laser pulse with a finite slab. Analyses were performed to define high-energy laser effects on solids. A variety of convective boundary conditions were applied to the solution. Variation in thermal response of the solids was established for a number of slab thicknesses and external cooling characteristics due to airflow over the heated surface. It was found that both surface convection and material properties affect the peak temperature location within the slab over time. In addition, the change in depth of the peak temperature increases for greater surface cooling.

Nomenclature

A	=	function, Eq. (5b)
c_p	=	specific heat, J/kg · K
F	=	initial temperature, K
$\bar{F}$	=	function, Eq. (5c)
$\dot{g}'''$	=	energy generation rate per unit volume, W/m^3
$\dot{g}(t)$	=	laser source temporally decaying portion, Eq. (2e)
$\dot{g}(x)$	=	laser source spatially decaying portion, Eq. (2d)
$\bar{g}(\beta_m, t')$	=	function, Eq. (5d)
H	=	ratio of convection heat transfer coefficient to thermal conductivity, h/k
h	=	convective heat transfer coefficient, W/m^2 · K
I_o	=	laser peak power density, W/m^2
k	=	thermal conductivity, W/m · K
L	=	thickness of the slab, m
N	=	normalization integral
n	=	real part of the refractive index
R	=	surface reflectivity
T	=	temperature, K
T_∞	=	external environment temperature, K
T_0	=	initial temperature, K
t	=	time, ns
X	=	eigenfunction
x	=	x coordinate
α	=	thermal diffusivity, m^2/s
β	=	eigenvalue
δ	=	laser pulse fall-time parameter, s^{-1}
ε	=	emissivity
θ	=	laser pulse rise-time parameter, s^{-1}
κ	=	imaginary part of the refractive index
λ	=	wavelength, nm
μ	=	absorption coefficient, m^{-1}
ρ	=	density, kg/m^3

Subscripts

m	=	index
1	=	incident surface, surface 1
2	=	nonincident surface, surface 2

Dimensionless Parameters

Bi	=	Biot number, $h/\mu k$
T^*	=	temperature, $(T - T_0)/[I_0(1 - R)/\mu k]$
$T^*_{\max}$	=	maximum temperature within the slab
x^*	=	distance, μx
$x^*_{T_{\max}}$	=	value of x^* at maximum temperature
τ	=	time, $t\alpha\mu^2$

I. Introduction

THE effects of laser heating in solids are of interest in a variety of engineering applications, such as laser processing of materials [1] (including semiconductors [2]), phase change processes [3], material removal [4], and high-power laser impingement on a blunt enclosure in a high-speed flow [5]. In all applications, accurately controlling the temperature profile within the material as a function of time is desired. Predicting the response of an affected surface requires realistic characterization of not only the heat transfer within the medium, but also of the laser pulse itself [6].

Models exist that simulate laser heating of a semi-infinite medium with a variety of heating profiles and cooling effects. Ready [7] studied the effects of high-power laser incidence on absorbing opaque surfaces. The study determined the temperature rise with no phase change and also investigated the vaporization process induced by a shorter, higher-power laser pulse. Dabby and Paek [8] analytically investigated the material removal process from the front surface of a solid heated by a high-intensity laser. The study revealed that for certain laser and material parameters subsurface temperatures exceeded the surface temperature. As a result, rapid and efficient explosive material removal process could occur. Blackwell [9] modeled the effect of continuous laser heating of a semi-infinite slab with convection on the surface of incidence. This analysis demonstrated that intense laser heating of a surface could result in catastrophic failure without melting or burning through the surface.

Presented as Paper 0981 at the 44th AIAA Aerospace Sciences Meeting and Exhibit, Reno, NV, 9–12 January 2006; received 9 February 2006; revision received 19 October 2006; accepted for publication 24 November 2006.

*Member of Technical Staff, Spacecraft Thermal Department, Vehicle Systems Division, Engineering and Technology Group, P.O. Box 92957, Mail Stop M4/908.

†Member of Technical Staff, Spacecraft Thermal Department, Vehicle Systems Division, Engineering and Technology Group, P.O. Box 92957, Mail Stop M4/916.

‡Director, Spacecraft Thermal Department, Vehicle Systems Division, Engineering and Technology Group, P.O. Box 92957, Mail Stop M4/908. Associate Fellow AIAA.

The study went further to explain the so-called "explosive removal of material" phenomenon suggested by Dabby and Paek [8]. The event could take place because a maximum temperature is present beneath the surface that is subjected to simultaneous heating and cooling. After a sufficient portion of the incident laser energy is absorbed by the solid body, there is a net gain of energy inside the solid while the boundary loses heat to the external environment. Chaudhry and Zubair [10] presented a closed-form analytical solution of temperature and heat flux distributions within a semi-infinite solid due to a spatially decaying, instantaneous laser source. Zubair and Chaudhry [11,12] investigated 1-D heat conduction in a semi-infinite solid for both a time-dependent laser source and an instantaneous spatially decaying laser source. Their time-dependent laser source decayed exponentially from an initial maximum. Yilbas [13] produced a closed-form solution for 1-D conduction in a semi-infinite medium subjected to a laser pulse. The pulse definition more closely approximated the time variance of a real laser. All of the aforementioned studies were limited to semi-infinite solids; therefore, transient analytical solutions were possible with the aid of the classical Laplace transform technique.

The goal of the present analysis is to provide an improved model of laser heating at a surface by analyzing a spatially and temporally decaying laser pulse incident on a slab of finite thickness. The model determines the temperature distribution and the location of the maximum temperature within the solid. Results are provided in dimensionless form or normalized such that they are useful over a wide range of applications. A realistic set of parameters is used to describe the laser as well as the target material. The pulse is defined to be similar to a high-power laser appropriate for use in materials processing. The slab thickness and material properties are chosen such that the effect of laser heating on the temperature profile is clearly visible. Similar to Blackwell's study [9], the present analysis is useful in determining the location of maximum temperature, but does so for a finite slab. The results presented emphasize the effect of material properties and surface cooling on the thermal response.

II. Physical Problem Formulation

Heat conduction in a finite slab irradiated by a spatially and temporally decaying laser source with convective cooling on both sides is analyzed, as shown in Fig. 1. It is assumed that the slab has uniform thickness and constant material properties. At $t = 0$, the temperature field within the slab is defined as $T = F(x)$. For $t > 0$, surface 1 is irradiated by a laser. A portion of the laser energy is reflected away while the remaining energy is absorbed and then conducted by the material. At $t > 0$, the slab dissipates heat by convection from its boundary surfaces to an environment at T_∞.

The energy equation governing heat conduction in a one-dimensional finite region with internal energy generation can be formulated as

$$k\frac{\partial^2 T(x,t)}{\partial x^2} + \dot{g}'''(x,t) = \rho c_p \frac{\partial T(x,t)}{\partial t} \quad \text{in } 0 < x < L, \qquad t > 0 \tag{1}$$

where $\dot{g}'''$ denotes the energy generation rate per unit volume inside the absorbing material. Because this is a one-dimensional problem, variation in laser intensity (I_o) is not considered in the plane normal to the beam. The internal heat generation term can be a function of both time and space. For laser applications, the internal energy source term can be written as [6]

$$\dot{g}'''(x,t) = I_o \mu (1-R)\dot{g}(t)\dot{g}(x) \tag{2a}$$

where I_o is the laser incident intensity. R is the surface reflectivity of the solid dependent on the wavelength of the incident laser, and μ is the absorption coefficient, given by

$$R = \frac{(n-1)^2 + \kappa^2}{(n+1)^2 + \kappa^2} \tag{2b}$$

$$\mu = \frac{4\pi\kappa}{\lambda} \tag{2c}$$

The spatially and temporally decaying portions of the source term are given by

$$\dot{g}(x) = e^{-\mu x} \tag{2d}$$

$$\dot{g}(t) = e^{-\theta t} - e^{-\delta t} \tag{2e}$$

where θ and δ are laser pulse parameters. Equations (2d) and (2e) represent the spatial variation (penetration) within the solid and the temporal variation of the laser output pulse, respectively. The exponential function designated by Eq. (2e) accounts for the rise and fall times of the laser pulse. The laser beam parameters chosen for this analysis are as follows: wavelength = 1000 nm; $I_o = 24$ GW/cm^2, the maximum pulse peak power density; pulse length = 25 ns, FWHM; $\theta = 4.9 \times 10^7$ 1/s; and $\delta = 2.45 \times 10^8$ 1/s. The parameters were approximately based on the characteristics of a Lambda Physik Powergator PG1064-30 laser and used a pulse parameter ratio $\theta/\delta = 1/5$ (Yilbas [13]). The temporal profile of the laser, $\dot{g}(t)$, is illustrated in Fig. 2.

As stated previously, both boundary surfaces dissipate heat to the environment at temperature T_∞; thus, the boundary conditions at these two surfaces take the form

$$k\frac{\partial T}{\partial x} = h_1(T - T_\infty) \quad \text{at } x = 0, \qquad t > 0 \tag{3a}$$

$$-k\frac{\partial T}{\partial x} = h_2(T - T_\infty) \quad \text{at } x = L, \qquad t > 0 \tag{3b}$$

and the assumed initial condition is a uniform temperature

$$T = F(x) \quad \text{for } t = 0, \quad \text{in } 0 \le x \le L \tag{4}$$

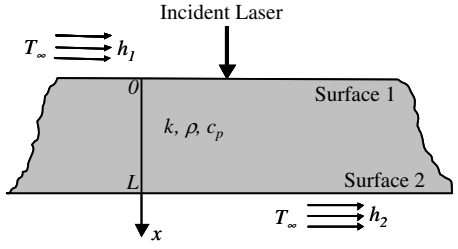

Fig. 1 Schematic of a finite slab subjected to spatially and temporally decaying laser heating.

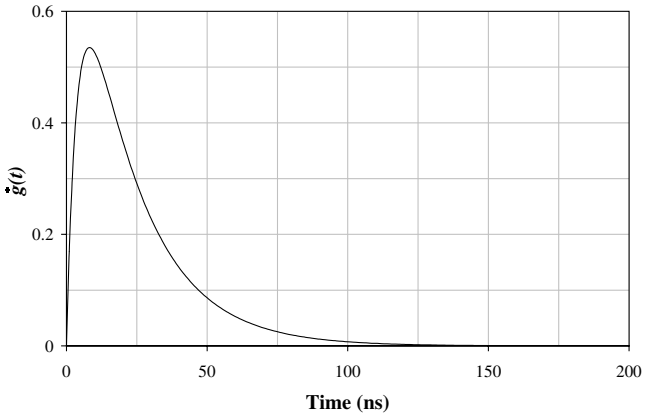

Fig. 2 Temporal function of the laser pulse.

III. Heat Conduction with Internal Energy Generation

It is well known that the method of separation of variables is suitable for the solution of a large class of partial differential equations of heat conduction. However, the use of an integral transform is easier when the equation and the boundary conditions involve nonhomogeneities. The integral-transform technique provides a systematic, efficient, and straightforward approach for the solution of linear, homogeneous, or nonhomogeneous, and steady-state or time-dependent boundary-value problems of heat conduction. As the governing equation and boundary conditions of the physical problem fall within this class of heat conduction, the integral-transform technique is an appropriate method to obtain the temperature distribution. A general solution of Eq. (1) has been developed by Özisik [14] by using this technique, which can be readily written as

$$T(x,t)=\sum_{m=1}^{\infty}\frac{X(\beta_m,x)}{N(\beta_m)}e^{-\alpha\beta_m^2 t}\left[\bar{F}(\beta_m)+\int_0^t e^{\alpha\beta_m^2 t'}A(\beta_m,t')\,\mathrm{d}t'\right] \tag{5a}$$

where

$$A(\beta_m,t')=\frac{\alpha}{k}\bar{g}(\beta_m,t') \tag{5b}$$

$$\bar{F}(\beta_m)=\int_0^L X(\beta_m,x')F(x')\,\mathrm{d}x' \tag{5c}$$

$$\bar{g}(\beta_m,t')=\int_0^L X(\beta_m,x')\dot{g}'''(x',t')\,\mathrm{d}x' \tag{5d}$$

In the above equations, the eigenfunctions $X(\beta_m,x)$, the normalization integral $N(\beta_m)$, and the eigenvalues are readily obtainable for various combinations of the boundary conditions [14]. The normalization integral is related to the eigenfunction in the following form:

$$N(\beta_m)=\int_0^L [X(\beta_m,x')]^2\,\mathrm{d}x' \tag{6}$$

IV. Solution of the Physical Problem

For the physical problem under consideration, if both boundary surfaces of the slab dissipate heat by convection to an environment at zero temperature ($T_\infty=0$) and the slab is initially at a uniform temperature of 0°C [$F(x)=0$], it is possible to write the solution from Eq. (5) by setting [14]

$$X(\beta_m,x)=\beta_m\cos(\beta_m x)+H_1\sin(\beta_m x) \tag{7a}$$

$$N(\beta_m)=\frac{1}{2}\left[(\beta_m^2+H_1^2)\left(L+\frac{H_2}{\beta_m^2+H_2^2}\right)+H_1\right] \tag{7b}$$

where H_1 and H_2 are h_1/k and h_2/k, respectively. The terms β_m in the above equations are the eigenvalues (positive roots) of the equation

$$\tan\beta_m L=\frac{\beta_m(H_1+H_2)}{\beta_m^2-H_1H_2} \tag{8}$$

which is specific to the chosen boundary conditions. Based on the aforementioned assumptions and boundary condition [Eq. (3)], the temperature distribution within the slab is represented in analytical form as

$$T(x,t)=\sum_{m=1}^{\infty}\frac{2\alpha}{k(\theta-\alpha\beta_m^2)(\delta-\alpha\beta_m^2)\{(\beta_m^2+H_1^2)[L+H_2/(\beta_m^2+H_2^2)]+H_1\}}[\delta-\theta+(\theta-\alpha\beta_m^2)e^{\alpha\beta_m^2 t-\delta t}-(\delta-\alpha\beta_m^2)e^{\alpha\beta_m^2 t-\theta t}]\mu I_o(1$$
$$-R)[\beta_m\cos(\beta_m x)+H_1\sin(\beta_m x)]e^{-\alpha\beta_m^2 t}\int_0^L X(\beta_m,x)e^{-\mu x}\,\mathrm{d}x \tag{9a}$$

where

$$\int_0^L X(\beta_m,x)e^{-\mu x}\,\mathrm{d}x=\frac{\mu\beta_m+H_1\beta_m-\beta_m e^{-\mu L}[(\mu+H_1)\cos(\beta_m L)-(\beta_m-\frac{H_1\mu}{\beta_m})\sin(\beta_m L)]}{\mu^2+\beta_m^2} \tag{9b}$$

V. Results and Discussion

An analytical solution [Eq. (9)] for the temperature distribution within a slab subjected to a time-dependent laser pulse is obtained using the integral-transform technique. To determine the influence of convective cooling on the location of maximum temperature, the convection coefficient for each side of the slab is varied by alternating the Biot number. As the maximum temperature location is a function of both external cooling and material properties, results are generated for a range of Biot numbers, which are defined as the ratios of surface convection to slab conduction. The material properties are assumed to be constant for this study. Thus, Biot numbers and convective heat transfer coefficients are directly proportional. Four Biot numbers were selected for the laser incident surface (surface 1) while the Biot numbers for the opposite surface

Table 1 Combination of Biot numbers used at surfaces 1 and 2

	Biot no.			
Surface 1 (laser incidence)	0.5	1.0	2.0	5.0
Surface 2 (opposite)	~0, 0.5, 1.5	~0, 1.0, 3.0	~0, 2.0, 6.0	~0, 5.0, 15.0

(surface 2) were represented by three cases, which are defined as follows: case 1: $Bi_2 \approx 0$; case 2: $Bi_2 \approx Bi_1$; and case 3: $Bi_2 \approx 3Bi_1$. The combinations of Biot numbers are summarized in Table 1.

Although all of the cases have convection at the boundaries, a nearly adiabatic condition was assigned to surface 2 by using a small convective heat transfer coefficient (50 $\mathrm{W/m^2 \cdot K}$), which equates to a Biot number of 6.47×10^{-5}. By coupling the near adiabatic case with a large Biot number on surface 1, the effect of laser heating on the outside of a blunt enclosure in a high-speed flow can be simulated.

The numerical solution of Eq. (9) was implemented in *Maple* [15] while the eigenvalues [Eq. (8)] were determined by exercising a code developed in MATLAB [16], which used the Newton–Raphson root-finding method. The temperature distribution designated by Eq. (9) was obtained as a series solution. The series solution was evaluated by successively increasing the number of terms until additional terms did not significantly alter the temperature profile (i.e., the change in temperature divided by the number of additional terms was less than 1×10^{-4}). In all cases, at least 100 terms were needed. Smaller times scales, such as $\tau = 5 \times 10^{-5}$, require a greater number of terms, approximately 200.

To gain a better understanding of the relationship between the location of maximum temperature and convective cooling, the analytical solution [Eq. (9)] was exercised for a silicon slab of finite thickness. The thermophysical and optical properties used for the simulation are as follows: $k = 156$ $\mathrm{W/m \cdot K}$; $\rho = 2330$ $\mathrm{kg/m^3}$; $c_p = 713$ $\mathrm{J/kg \cdot K}$; $\mu = 4952.65$ 1/m; and $R = 0.3186$ [17,18].

With the ability to model a finite slab, convective cooling could be considered at surface 2. However, to clearly observe the influence of convection and laser heating on the temperature profile, the slab thickness had to be chosen based on the optical properties of the material. By selecting two slab thicknesses, one less than and one much greater than $1/\mu$, two regimes of energy deposition could be observed. For a thickness of 0.1 mm (less than $1/\mu$), a portion of the incident energy is transmitted through the slab; for a thickness of 1 mm (much greater than $1/\mu$), all of the incident energy is absorbed within the slab.

The temperature profile within the slab was determined at increasing time intervals to capture the transient heating and cooling of the medium. Figures 3 and 4 depict the temperature profiles for slab thicknesses of 0.1 and 1 mm, respectively, for case 1 conditions.

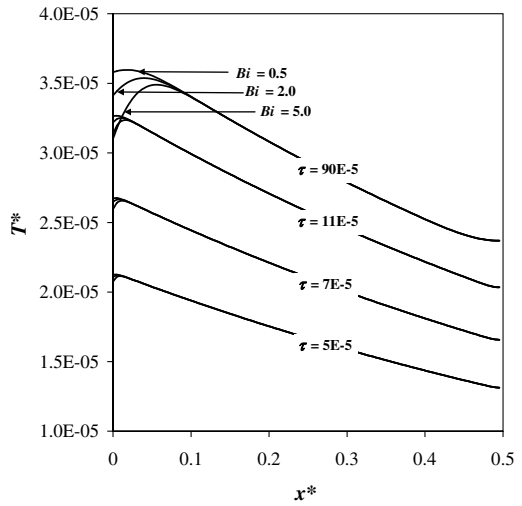

Fig. 3 Case 1: Dimensionless temperature profile as a function of x^* for various Biot numbers and τ (0.1 mm slab).

Notice that the peak temperature is located inside the slab rather than at the surface because convection lowers the temperature at surface 1. Convective cooling becomes more pronounced with increasing Biot number and time. The temperature peaks are more noticeable for larger Biot numbers because in this study greater Biot numbers are equivalent to higher convection coefficients. Producing a temperature profile that clearly exhibits a peak temperature requires large Biot numbers. For example, a convection coefficient of 3.9246×10^6 $\mathrm{W/m^2 \cdot K}$ results in a Biot number of 5.0.

Observe that the temperature distribution is noticeably different for the 0.1 and 1 mm slabs. The temperature gradient from surface 1 to surface 2 is significantly larger for the 1 mm slab. The larger temperature gradient occurs because surface 2 remains at its initial temperature for a 1 mm slab; the incident energy does not reach surface 2. For a 0.1 mm slab the incident energy penetrates the thickness of the slab, raising the temperature of surface 2. Recall that for case 1, the boundary condition at surface 2 resembles a near adiabatic interface, which is observed in Fig. 3 by a temperature profile slope that approaches zero. When an appreciable convective heat transfer coefficient is applied to surface 2, as defined by cases 2 and 3, the temperature profile slope is significantly greater, which can be seen in Figs. 5 and 6. Cases 2 and 3 temperature profiles for a 1 mm slab are not shown because they are identical to those shown in Fig. 4. The profiles are identical because the incident energy does not impact the temperature on surface 2, and thus, surface 2 boundary conditions do not affect the temperature profile.

The maximum temperature location history for four Biot numbers is provided in Fig. 7. As expected, the peak temperature translation rate is directly proportional to the Biot number. The time history for the maximum peak temperature inside a 0.1 mm slab for case 2 with $Bi_1 = 5$ and $Bi_2 = 5$ is presented in Fig. 8. The peak temperature rises while the energy provided by the laser is greater than that loss by convection. The temperature plateaus when the amount of energy being absorbed by the material equals the energy loss due to convection. This occurs near the end of the laser pulse, approximately at $\tau = 2.5 \times 10^{-4}$.

Although the previous discussions provide insight regarding the spatial temperature profile through the slab, the temporal relationship between peak temperature location and its corresponding temperature has not been presented. To address this topic, the maximum temperature and its location were tracked with time for case 2 boundary conditions. The data are plotted in Figs. 9 and 10 for slab thicknesses of 0.1 and 1 mm, respectively. To provide a sense of how

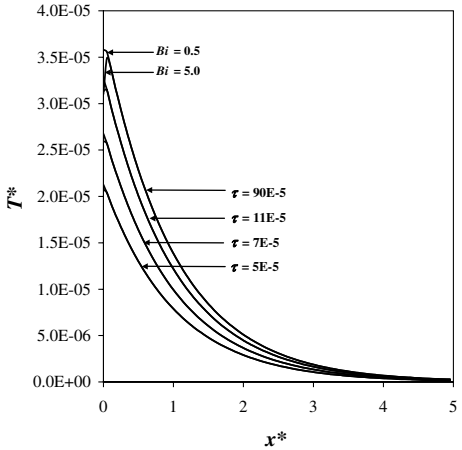

Fig. 4 Case 1: Dimensionless temperature profile as a function of x^* for various Biot numbers and τ (1 mm slab).

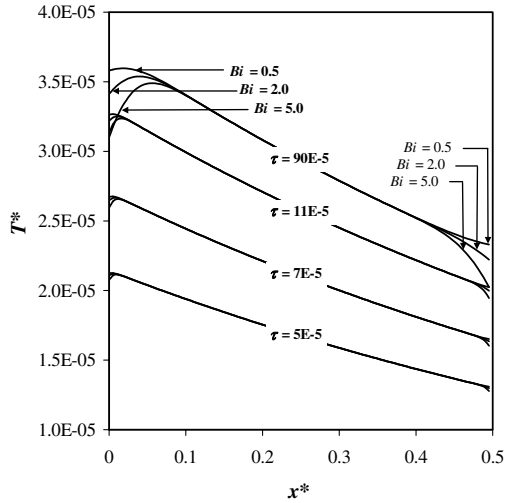

Fig. 5 Case 2: Dimensionless temperature profile as a function of x^* for various Biot numbers and τ (0.1 mm slab).

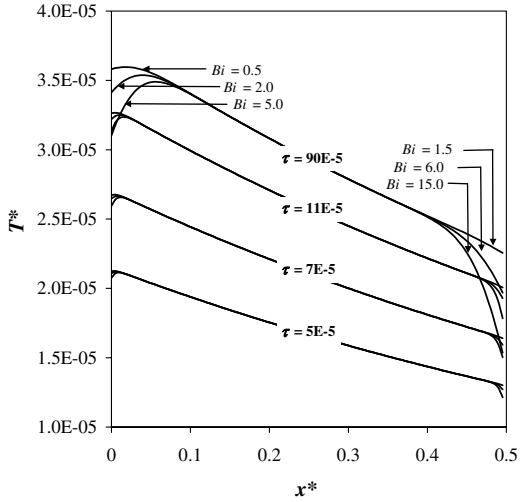

Fig. 6 Case 3: Dimensionless temperature profile as a function of x^* for various Biot numbers and τ (0.1 mm slab).

the location of peak temperature changes with time, dimensionless intervals are marked on each plot.

The temperature peaks in Figs. 9 and 10 indicate when the amount of energy being absorbed from the laser has decreased to the point that it is equal to the amount of heat being removed by convection. This is the same phenomenon seen in Fig. 8. The time it takes to reach the peak (roughly 125 ns) is approximately the same for both curves, as it is primarily dependent on the laser pulse profile. As a side note,

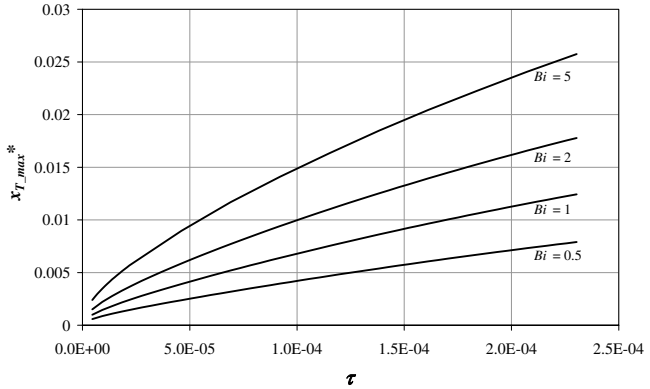

Fig. 7 Dimensionless depth to where maximum temperature occurs as a function of τ for various Biot numbers.

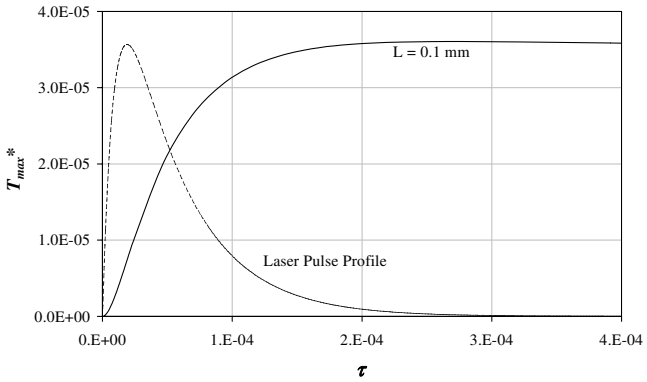

Fig. 8 Dimensionless maximum temperature as a function of τ during the laser pulse.

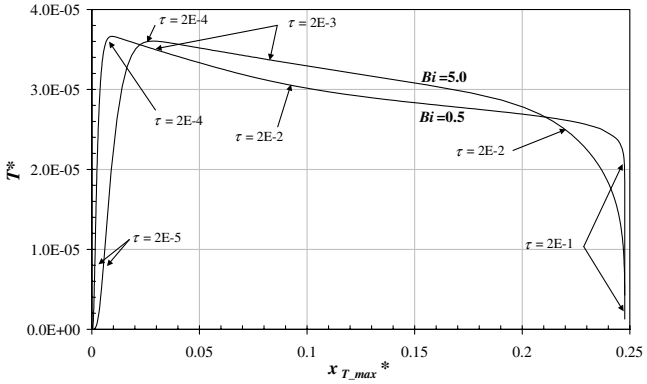

Fig. 9 Dimensionless temperature as a function of the depth at which maximum temperature occurs for increasing time intervals (0.1 mm thickness).

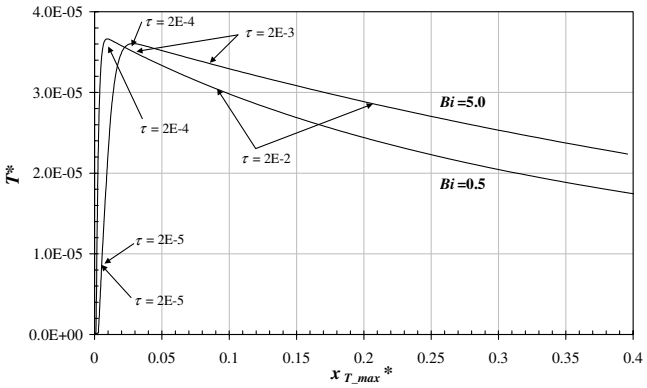

Fig. 10 Dimensionless temperature as a function of the depth at which maximum temperature occurs for increasing time intervals (1 mm thickness).

125 ns is equal to 5 times the full width at half maximum of the laser pulse and is very near the end of the laser pulse, as can be seen in Fig. 2. For the same reason that the maximum temperature was more distinct in Figs. 3, 5, and 6 for greater Biot numbers, the maximum temperatures in Figs. 9 and 10 are slightly lower for greater Biot numbers.

Shortly after the peaks in Figs. 9 and 10, the maximum temperature location is solely driven by convection on surface 1; the laser is no longer impinging the surface. As the slab cools, the profiles for the two slab thicknesses begin to differ. For a 0.1 mm slab, the temperature at surface 2 is much greater than the surrounding temperature; thus, convective cooling plays an important role. Because the convective heat transfer coefficient is the same on both sides of the slab ($Bi_1 = Bi_2$), the maximum temperature location

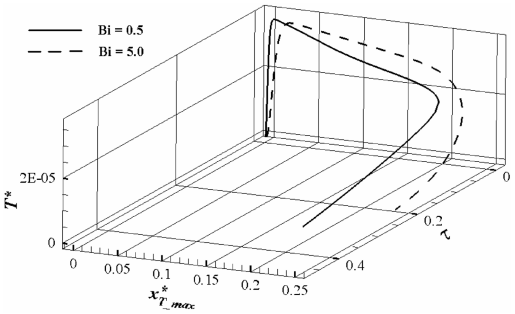

Fig. 11 3-D plot: Dimensionless temperature as a function of the depth at which maximum temperature occurs for increasing time intervals (0.1 mm thickness).

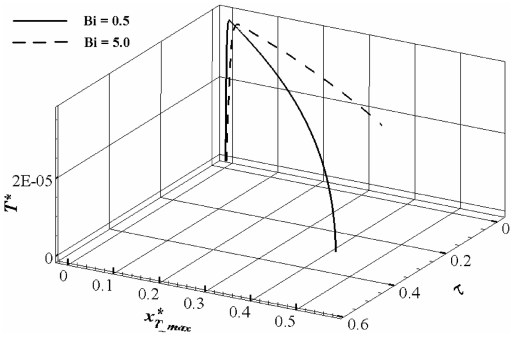

Fig. 12 3-D plot: Dimensionless temperature as a function of the depth at which maximum temperature occurs for increasing time intervals (1.0 mm thickness).

moves asymptotically to the middle of the slab ($x^* = 0.25$). Then, the slab is symmetrically cooled to equilibrium with the surrounding environment. For a 1 mm slab, the incident energy is absorbed in only a portion of the material depth due to its relative thickness as compared to the absorption coefficient. Therefore, the temperature at surface 2 remains at its initial temperature, which is the same as the surrounding temperature. As a result, the cooling on surface 1 forces the peak temperature location all the way to surface 2. This phenomenon can be envisioned even though it is not shown on the graph. Three-dimensional representations of Figs. 9 and 10 are provided in Figs. 11 and 12, respectively, and offer a different perspective.

To further investigate the effect of slab thickness on peak temperature within the slab, a dimensionless maximum temperature time history is provided in Fig. 13 for case 1 boundary conditions and $Bi_1 = 5$. The profiles are initially the same because the curve is defined by the laser pulse and material optical properties. Only after the laser pulse has ended do the profiles begin to differ. While the laser is off and the slab is being cooled by convection only, the

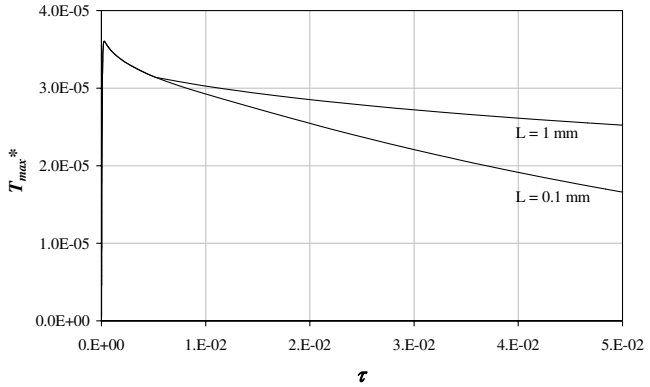

Fig. 13 Dimensionless maximum temperature as a function of τ for $Bi = 5$ and case 1 boundary conditions.

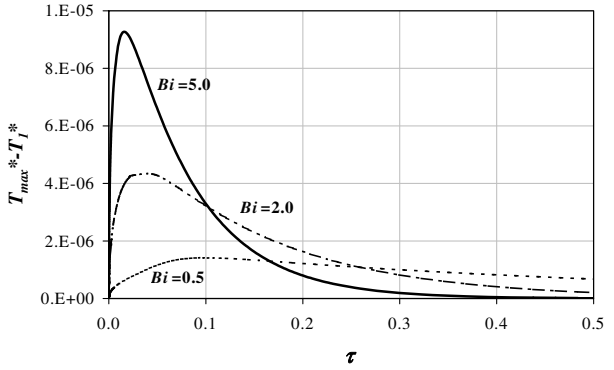

Fig. 14 Difference between surface 1 temperature and maximum temperature as a function of τ for different Biot numbers.

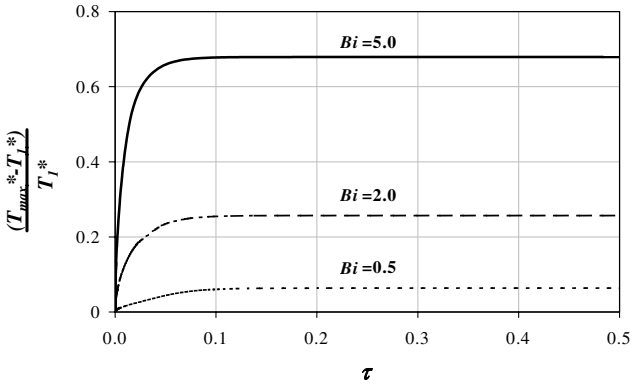

Fig. 15 Normalized difference between surface 1 temperature and maximum temperature as a function of τ for different Biot numbers.

characteristic length is defined by half of the slab's thickness. Thus, the effective cooling rates for the two slabs differ.

The difference between surface 1 temperature and maximum temperature as a function of τ for different Biot numbers is presented in Fig. 14 for case 2 boundary conditions. For large Biot numbers, convection dominates the heat transfer process. A surface with a larger Biot number yields a greater difference between the surface temperature and the maximum peak temperature. This phenomenon is clearly demonstrated in Fig. 14 as the value of the Biot number decreases from 5 to 0.5. A slightly different perspective is provided by normalizing the temperature gradient by the temperature at surface 1 as shown in Fig. 15. The plateau in the profile signifies that after the laser pulse has ended the temperature gradient decreases directly with the temperature at surface 1.

VI. Summary

An analytical expression for the temperature distribution within a slab subjected to spatially and temporally decaying laser heating at one of its external surfaces has been developed and solved for various boundary cooling conditions. The method and transient results can be used to determine the temperature profile within a material sample for a variety of engineering applications. The model improves upon past models by combining a realistic laser pulse profile with a material sample of finite thickness. Earlier models in this area dealt mainly with semi-infinite media and constant or decaying laser pulses. The results from those studies would have limited practical applications.

In all cases considered in this work, the shape of the temperature profile is such that the peak occurs inward from the surface at all times, a result consistent with earlier investigations. Convection at the two surfaces and material properties both affect the location of the peak over time. As the Biot number associated with either surface is made larger, the prominence of the peak increases with respect to the temperature at the surface of incidence. Furthermore, the movement

of the location of peak temperature away from the surface of incidence occurs more rapidly for larger Biot numbers.

The work reported in this study was for convective cooling only. However, most realistic problems encountered in high temperature engineering applications involve radiative cooling and temperature-dependent material properties. The model is being expanded to include these factors and the results will be available in future studies.

References

[1] Metev, S. M., and Veiko, V. P., *Laser-Assisted Microtechnology*, Springer–Verlag, Berlin, 1994, Chap. 4.

[2] Chen, J. K., Tzou, D. Y., and Beraun, J. E., "Numerical Investigation of Ultrashort Laser Damage in Semiconductors," *International Journal of Heat and Mass Transfer*, Vol. 48, Nos. 3–4, 2005, pp. 501–509.

[3] Lundell, J. H., and Dickey, R. R., "Vaporization of Graphite in the Temperature Range of 4000 to 4500 K," AIAA Paper 76-166, 26–28 January 1976.

[4] Kemp, N. H., "Effect of Melt Removal by Aerodynamic Shear on Melt-Through of Metal Plates," *AIAA Progress in Astronautics and Aeronautics*, AIAA, New York, 1978, Vol. 59, pp. 225–260.

[5] Robin, J. E., and Nordin, P., "Enhancement of CW Laser Melt-Through of Opaque Solid Materials by Supersonic Transverse Gas Flow," *Applied Physics Letters*, Vol. 26, No. 6, 1975, pp. 289–292.

[6] Ready, J. F., *Industrial Applications of Lasers*, Academic Press, New York, 1978.

[7] Ready, J. F., "Effects Due to Absorption of Laser Radiation," *Journal of Applied Physics*, Vol. 36, No. 2, 1965, pp. 462–468.

[8] Dabby, F. W., and Paek, U.-C., "High-Intensity Laser-Induced Vaporization and Explosion of Solid Material," *IEEE Journal of Quantum Electronics*, Vol. QE-8, No. 2, 1972, pp. 106–111.

[9] Blackwell, B. F., "Temperature Profile in Semi-infinite Body With Exponential Source and Convective Boundary Condition," *Journal of Heat Transfer*, Vol. 112, No. 3, 1990, pp. 567–571.

[10] Chaudhry, M. A., and Zubair, S. M., "Conduction of Heat in a Semi-Infinite Solid with an Exponential-Type Initial Temperature Profile: Temperature and Heat Flux Solutions due to an Instantaneous Laser Source," *Wärme- und Stoffübertragung*, Vol. 30, No. 1, 1994, pp. 41–46.

[11] Zubair, S. M., and Chaudhry, M. A., "Heat Conduction in a Semi-Infinite Solid When Subjected to Spatially Decaying Instantaneous Laser Source," *Wärme- und Stoffübertragung*, Vol. 28, No. 7, 1993, pp. 425–431.

[12] Zubair, S. M., and Chaudhry, M. A., "Heat Conduction in a Semi-Infinite Solid due to Time-Dependent Laser Source," *International Journal of Heat and Mass Transfer*, Vol. 39, No. 14, 1996, pp. 3067–3074.

[13] Yilbas, B. S., "A Closed Form Solution for Temperature Rise Inside Solid Substrate due to Time Exponentially Varying Pulse," *International Journal of Heat and Mass Transfer*, Vol. 45, No. 9, 2002, pp. 1993–2000.

[14] Özisik, M. N., *Heat Conduction*, 2nd ed., Wiley, New York, 1993, Chap. 13.

[15] Maple 10, Maplesoft, Waterloo Maple, Inc., Canada, 2005.

[16] Matlab 6.1, The MathWorks, Inc., Natick, MA, 2001.

[17] American Society for Metals, *Metals Handbook*, Vol. 2, ASM International, Ohio, 1990.

[18] Palik, E. D., *Handbook of Optical Constants of Solids*, Academic Press, New York, 1985.